T^2 law for magnetite-based ferrofluids

2003 J. Phys.: Condens. Matter 15 765

(http://iopscience.iop.org/0953-8984/15/6/303)

INSTITUTE OF PHYSICS PUBLISHING JOURNAL OF PHYSICS: CONDENSED MATTER

J. Phys.: Condens. Matter **15** (2003) 765–776 PII: S0953-8984(03)55199-2

T^2 law for magnetite-based ferrofluids

C Caizer

Department of Electricity and Magnetism, West University of Timisoara, Bd. V Parvan no 4, 1900 Timisoara, Romania

E-mail: ccaizer@physics.uvt.ro

Received 24 October 2002
Published 3 February 2003
Online at stacks.iop.org/JPhysCM/15/765

Abstract

The temperature dependence of the saturation magnetization of Fe_3O_4 *surfacted* nanoparticles does not follow the law in T^2 that corresponds to bulk ferrite: $M_s(T) = M_s(0)[1 - BT^2]$ (where $M_s(T)$ is the saturation magnetization at temperature T, $M_s(0)$ is the saturation magnetization at 0 K and B is a constant that depends on the exchange integral). This abnormal behaviour was studied for a ferrofluid that contains magnetite particles covered in oleic acid (surfactant) in a carrier fluid (kerosene); the anomaly is attributed to modification of the superexchange interaction between the iron ions from the surface layer of the nanoparticles, a layer that is formed due to the presence of the surfactant. Taking into consideration the size distribution of the particles, according to magneto-granulometric measurements and transmission electron microscopy, we have shown that the thickness of the surface layer at a temperature of 300 K is $\langle\eta\rangle \cong 0.9$ nm. By adopting the 'core–shell' model we have shown that the layer at the particles' surface is paramagnetic at room temperature and it gradually becomes ferrimagnetically ordered as the temperature decreases. The consequence of this change is the increase of the mean volume of the nanoparticles' magnetic core where the spins are aligned due to the superexchange interaction from 1280 to 1910 nm^3 when the temperature decreases from 300 to 77 K.

1. Introduction

The magnetic properties of materials made up of nanometric particles (nanoparticles) are usually different from those of the bulk material [1–7]. Besides the shape of the nanoparticles, their finite dimension and single-domain magnetic structure, there are intrinsic properties that determine a certain magnetic behaviour of the material in an external field [8]. In the case of ferrimagnetic ionic compounds, the orientation of magnetic moments on the surface of the nanoparticles can be altered due to competition in the exchange interaction between the superficial ions that are in an incomplete coordination. It is well known that in these systems

the exchange interaction is performed through the oxygen ion O^{2-} (superexchange). This way, the absence of the oxygen ion at the surface or the presence of another atom (ion) in the form of an impurity leads to an interruption of the superexchange interaction between magnetic cations and thus induces surface spin disorder [9]. This spin disorder can alter significantly the magnetic properties of the nanoparticles, especially when the surface/volume ratio of the nanoparticles is high [10–12].

The spin wave model predicts a dependence of the (spontaneous) saturation magnetization M_s on the temperature T, which, in the range of low temperatures, has the following form [13]:

$$M_s(T) = A(1 - BT^{\alpha}) \tag{1}$$

where the parameter $A = M_s(0)$ is the saturation magnetization at 0 K and B is a constant whose value depends on the exchange integral J ($B \sim 1/J^{\alpha}$). The coefficient α generally takes the value of 3/2 (Bloch law), a value that is well verified experimentally both for bulk ferromagnetic materials (Fe, Ni) [14, 15] and for some spinel ferrites (e.g. $Mn_xFe_{3-x}O_4$; $0.2 \leqslant x \leqslant 2.0$ [13]). For fine particles and clusters some theoretical calculations, as well as some experimental results, have shown that the temperature exponent α is higher than 3/2, the value corresponding to the bulk material [16, 17]. However, Martinez *et al* [18] have demonstrated that, in the case of systems made up of γ-Fe_2O_3 nanoparticles, the saturation magnetization does indeed follow a law in $T^{3/2}$ up to room temperature. Recently, Morais *et al* [19] have studied an ionic ferrofluid containing $NiFe_2O_4$ particles with a diameter of 11.1 nm. They have then established that the temperature dependence of the saturation magnetization in the temperature range of 4.2–293 K deviates from the law corresponding to the bulk material; this deviation was attributed to the magnetic anisotropy. These results, together with others [20], show that the dependence M_s versus T—verified for the bulk material—does not always have to be verified for systems made up of nanoparticles, a behaviour that can be interpreted in several ways.

In the case of Fe_3O_4 bulk ferrite (magnetite), the law (1) is well verified for $\alpha = 2$ and it has the following form [13]:

$$M_s(T)_{Fe_3O_4} = M_s(0)_{Fe_3O_4}(1 - B_{Fe_3O_4}T^2) \tag{2}$$

where the saturation magnetization is

$$M_s(0)_{Fe_3O_4} = 8n_m(0)\,\mu_B/a_0^3 = 502.5 \times 10^3 \text{ A m}^{-1} \tag{3}$$

and

$$B_{Fe_3O_4} = 5.54 \times 10^{-7} \text{ K}^{-2}. \tag{4}$$

In equation (3), $n_m(0)$ is the number of Bohr magnetons ($\mu_B = 9.274 \times 10^{-24}$ A m^2) in the volume of the cubic elementary cell $V_0 = a_0^3$ (where $a_0 = 8.39$ Å is the crystalline lattice constant) at 0 K.

If the magnetite nanoparticles are, however, covered in oleic acid (an organic surfactant), it is well known that the acid is adsorbed on the particles' surface. For this reason, due to the interaction between the cations on the particles' surface (Fe^{2+} and Fe^{3+} ions) and the surfactant molecules (the oxygen ions at their polar end), a superficial layer (iron oleate) is formed at the surface [21, 22]. This layer is non-magnetic at room temperature. This paper focuses on the experimental study of the dependence M_{sat} versus T at low temperatures in the case of Fe_3O_4 nanoparticles covered with oleic acid and dispersed in kerosene (ferrofluid), as well as establishing the variation law for this case. Another aspect we have studied was the magnetic nature of the layer that is formed at the surface of the nanoparticles.

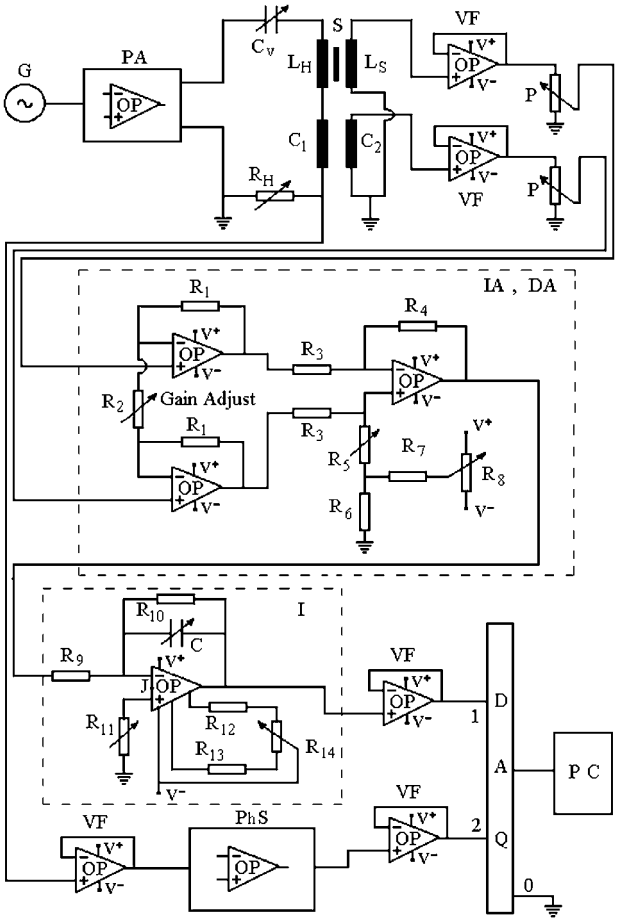

Figure 1. Schematic diagram of the experimental installation for recording the magnetization curves: G—generator, PA—power amplifier, OP—(low noise) operational amplifier, P—potentiometer, (IA, DA)—differential-input instrumentation amplifier with high input impedance adjustable gain, R_1, $R_2, \ldots$ —resistors, C_V, C—capacitors, J–OP—JFET input operational amplifier, V^+, V^-—supply voltage.

2. Experimental details

The *sample* we have used for studying the temperature dependence of the saturation magnetization of surfacted nanoparticles was a ferrofluid with Fe_3O_4 nanoparticles. The colloidal magnetite particles covered in oleic acid and dispersed in kerosene were obtained using the chemical coprecipitation method. After filtering and separation in a magnetic field we have obtained a ferrofluid with a narrow size distribution and good (steric) stability over time (as shown later on).

The *magnetic measurements* were made under quasistatic conditions (50 Hz) with the installation shown schematically in figure 1. The measurement of the magnetization was based on the fluxmeter method [23]. The ferrofluid (FF) in a test tube (S) of length 4.5 cm and diameter 4.5 mm was inserted into the probe coil (L_S) inside the magnetization coil (L_H). The component $\mu_0\vec{H}_e$ of the magnetic induction $\vec{B}$ ($\vec{B} = \mu_0\vec{H}_e + \mu_0\vec{M}$, where $\vec{M}$ is the magnetization and $\mu_0 = 4\pi \times 10^{-7}$ A m^{-1}), was compensated with a coil C_2 (situated inside the coil C_1) and

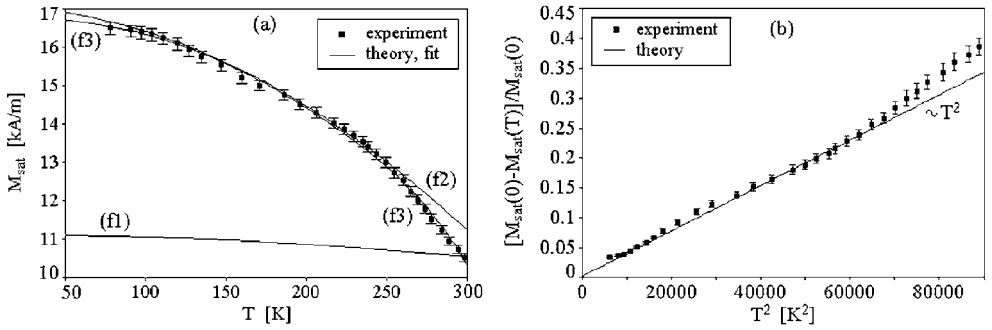

Figure 2. (a) Saturation magnetization as a function of temperature: experimental curve for surfacted nanoparticles (■); theoretical curve with the law in T^2 in agreement with equation (5) (f1), equation (1) (f2) and equation (22) (f3). (b) $[M_{sat}(0) - M_{sat}(T)]/M_{sat}(0)$ as a function of T^2.

two electronic circuits: the instrumentation amplifier (IA) and differential amplifier (DA). The high-order harmonics of the magnetization current were eliminated from the selective circuit C_v–L_H–C_1–R_H tuned to the frequency of the fundamental component (50 Hz). The DA output voltage signal (proportional to the time derivative of the sample's magnetization) is integrated by an electronic integrator (I). The voltage signal, which is proportional to the external magnetization field H_e, is picked up from the terminals of the precision resistor R_H. Both signals (1, 2) are then taken over by the data acquisition system (DAQ) connected to a personal computer (PC). In the *absence* of the FF sample, small signal phase delay corrections can be made with the phase shifter (PhS) or by using professional software. The signal inputs and outputs are separated by the voltage follower (VF). The FF sample, together with the probe coil L_S, are placed in a Teflon crucible that can be supplied with liquid nitrogen. The temperature was measured with a commercial Cu–(Cu/Ni) thermocouple. The demagnetizing field due to the sample's geometry $\vec{H}_d = -N_d\vec{M}$ (where N_d is the demagnetization factor) is corrected by a calculation program, so that the magnetization can be represented as a function of the field H from the sample ($H = H_e - H_d$). The installation was calibrated with Fe and Ni standards. The relative deviation of the saturation magnetization from the saturation magnetization of the standard is only 0.82%. During a measurement the magnetic field relative variation is less than 0.24%.

The *transmission electron microscopy (TEM)* of the ferrofluid sample was performed in a JEOL JEM-2010 electron microscope in order to determine the size distribution of the particles, and then their mean physical diameter.

The ferrofluid was frozen both in the presence of an external magnetic field ($H_{ext} = 1.1 \times 10^5$ A m^{-1}) that has saturated the sample, and in the absence of an external field, starting from room temperature down to the temperature of liquid nitrogen. In the absence of the field H_{ext} the particles were fixed by freezing with their easy magnetization axes statistically oriented in all directions. When the field H_{ext} was applied, the particles and, implicitly, their easy magnetization axes were oriented in the direction of the field, a direction that coincides with that subsequently measured. While the frozen system was returned to room temperature we recorded the magnetization curves at various temperatures.

3. Results and discussions

3.1. M_{sat} versus T

From the magnetization curves we have determined the saturation magnetization corresponding to the field 10^5 A m^{-1}. The values we have obtained in the absence of the field H_{ext} (■) are

shown in figure 2(a). The values obtained for the saturation magnetization when the sample was frozen in the presence of the field H_{ext} do not differ from the values obtained in the absence of the field. This means that the values measured for the saturation magnetization during cooling do not depend on the presence of the field H_{ext}, which induces uniaxial anisotropy. The figure shows that there is a pronounced increase of the saturation magnetization when the temperature decreases from 300 to 77 K. The relative increase of the sample's saturation magnetization is $\Delta M_{sat}/M_{sat300} = 57.1\%$ (where $\Delta M_{sat} = M_{sat77} - M_{sat300}$, M_{sat77} is the saturation magnetization at 77 K and M_{sat300} is the saturation magnetization at 300 K). This increase is much higher than the relative increase of the saturation magnetization of Fe_3O_4 bulk ferrite ($\Delta M_{sFe_3O_4}/M_{sFe_3O_4,300}$), which is of only ~6.6% [24] in the same temperature range. A similar behaviour was also observed for $Mn_{0.6}Fe_{0.4}Fe_2O_4$ nanoparticles surfacted with oleic acid and dispersed in kerosene [20].

Assuming that, in the case of the system made up of surfacted Fe_3O_4 nanoparticles, the saturation magnetization follows the law in T^2 the same way as in the case of bulk ferrite, according to equation (2), we have the function

$$M_{sat}(T) = 12.06 \times 10^3[1 - 5.54 \times 10^{-7}T^2]\ (\mathrm{A\ m^{-1}}), \tag{5}$$

represented by curve (f1) in figure 2(a). For the purpose of representation we have taken into account the magnetic packing fraction $\Phi_m = 0.024$ (as shown later on) in order to determine the saturation magnetization at 0 K. However, it can be observed that there is a very high deviation of curve (f1) from the experimental curve (■) that corresponds to the surfacted Fe_3O_4 nanoparticles. This deviation shows that a law of type (1) is not suitable to describe correctly the temperature dependence of the saturation magnetization of surfacted magnetite nanoparticles.

Fitting the experimental curve (■) with the function described by equation (1), and considering A and B as parameters, we obtain curve (f2) (full curve). In this case we can observe that curve (f2) is becoming closer to the experimental curve. However the values of the parameters A and B increase considerably compared to those corresponding to bulk Fe_3O_4 (A increases from 12.06×10^3 to 17.05×10^3 A m^{-1}, whereas B increases from 5.54×10^{-7} to 38.00×10^{-7} K^{-2}). Furthermore, a significant deviation from linearity can be observed in the representation $[M_{sat}(0) - M_{sat}(T)]/M_{sat}(0)$ versus T^2, as shown in figure 2(b). All these results suggest that the significant increase of the saturation magnetization of the system made up of surfacted nanoparticles with decreasing temperature has another cause other than the variation of the spontaneous magnetization with temperature.

If we take into consideration that the saturation magnetization of the ferrofluid is

$$M_{sat} = nm_p \tag{6}$$

where n is the (constant) concentration of the nanoparticles, we believe that the reason for the significant increase of the saturation magnetization must be the increase of the magnetic volume V_m (attached to the particles' cores), which determines the increase of the magnetic moment $m_p = M_s V_m$ of the nanoparticles. In order to clarify this issue, we have determined the mean magnetic diameter and the mean physical diameter of the nanoparticles in the ferrofluid, by taking into consideration the size distribution of the particles in the real system. Furthermore, for a rigorous determination of the magnetic diameter we have also taken into consideration the dependence of the particles' magnetic moment on the distribution of the magnetic diameters.

3.2. Mean magnetic diameter

Figure 3 shows the magnetization curve of the ferrofluid at room temperature (300 K). Fitting the curve with the function [25]

$$M(H, T) = M_{sat}L(H, T) \tag{7}$$

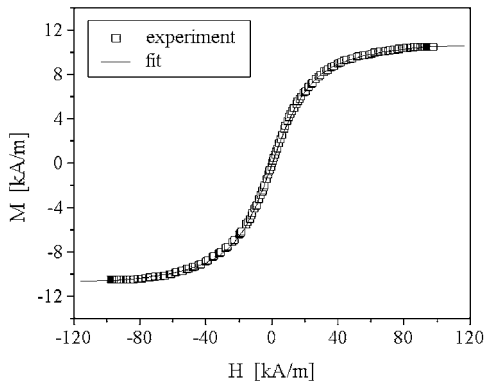

Figure 3. Magnetization curve at room temperature.

where

$$L(H, T) = \coth(\beta H/T) - T/(\beta H) \tag{8}$$

and

$$\beta = \mu_0 m_p / k_B \tag{9}$$

(where M_{sat} is the saturation magnetization of the ferrofluid, $L(H, T)$ is the Langevin function that depends on the field H and the temperature T and k_B is Boltzmann's constant), we can observe that the theoretical curve does overlap with the experimental points (□). The result shows that the ferrofluid has a superparamagnetic (SPM) behaviour. This behaviour is also caused by the relatively low magnetic packing fraction $\Phi_m = M_{sat}/M_s = 0.024$ ($M_s = 477.5 \times 10^3$ A m^{-1} [26]), which means that the distance between the particles is sufficiently big and thus the interactions between them are negligible. Indeed, the value of the coupling parameter γ, given by the ratio between the maximum interaction energy of the magnetic moments (m_p) of two particles approximated as being spherical (when the magnetic moments are in the same direction with the line that crosses the particles' centre) and the thermal energy $k_B T$ [27, 28]:

$$\gamma = \frac{\pi \mu_0 M_s^2}{144 k_B T} \left[\frac{(\langle d \rangle - 2\langle \eta \rangle)^2}{(\langle d \rangle + 2\delta)} \right]^3 \tag{10}$$

(in SI), has a value of $0.54 < 1$. In equation (10), δ is the chain length of the oleic acid molecule ($\sim$2 nm) and $\langle d \rangle$ and $\langle \eta \rangle$ is the mean diameter and mean thickness, respectively, of the layer on the particle surface ($\langle d \rangle = 12.7$ nm and $\langle \eta \rangle = 0.9$ nm, as shown in section 3.3). Previous studies have shown that particle clusters (chains) that are thermodynamically stable are formed for values of $\gamma > 1$ that are closer to the values 2–4.5 [29–31]. In our case, the obtained result ($\gamma = 0.54$) shows that the dipole–dipole interaction energy is sensibly lower than the thermal energy and, thus, the thermal agitation is successfully opposed to the formation of particle clusters. Thus, the presence of clusters in the ferrofluid is negligible.

If we take into consideration the size distribution of the particles' diameters according to a log-normal function (as suggested by O'Grady and Bradbury [32], and which is well verified experimentally [33, 34]), as well as the dependence of the magnetic moment m_p on the magnetic diameter d_m of the particle (equation (6)):

$$m_p = \pi M_s d_m^3 / 6 \tag{11}$$

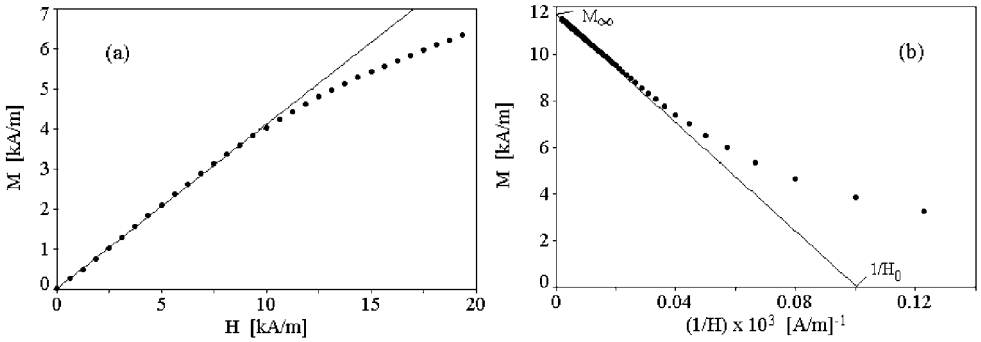

Figure 4. (a) M versus H in low fields and (b) M versus $1/H$ in high fields.

(in the approximation of spherical particles), the more precise relation for the magnetization of the nanoparticle system will be

$$M(H, T, d_m) = n \int_0^\infty m_p(d_m) L[\xi(H, T, d_m)] f(d_m)\, \mathrm{d}(d_m). \tag{12}$$

In equation (12)

$$f(d_m) = 1/(\sqrt{2\pi}\lambda_m d_m) \exp\{-[\ln(d_m) - \ln(d_{m0})]^2/2\lambda_m^2\} \tag{13}$$

is the distribution function [35] (where λ_m and d_{m0} are the distribution parameters and $\ln(d_{m0}) = \langle \ln(d_m) \rangle$, where $\langle \cdots \rangle$ is the mean). In the approximation of low and high fields, if we expand in series the Langevin function $L(\xi)$ for a low argument $\xi \ll 1[L(\xi) \to (1/3)\xi]$ and a high argument $\xi \gg 1[L(\xi) \to 1 - 1/\xi]$, respectively, and if we solve the integral equation (12), we obtain the mathematical expressions of the distribution parameters:

$$d_{m0} = \left[\frac{6k_B T}{\mu_0 \pi M_s H_0} \left(\frac{M_0}{3\chi_i H_0} \right)^{1/2} \right]^{1/3}, \qquad \lambda_m = \frac{1}{3} \left[\ln\left(\frac{3\chi_i H_0}{M_0} \right) \right]^{1/2}. \tag{14}$$

The initial susceptibility $\chi_i = 0.42$ results from the slope in the origin of the magnetization curve (figure 4(a)). $M_0 = 11.67 \times 10^3$ A m^{-1} and $H_0 = 10.00 \times 10^3$ A m^{-1} result from the extrapolation of the linear portion of the curve M–$1/H$ in the saturation domain (figure 4(b)). If we replace the values that resulted from equation (14), we obtain the mean magnetic diameter at a temperature of 300 K:

$$\langle d_m \rangle_{300} = d_{m0} \exp(\lambda_m^2/2) = 10.86 \pm 9 \times 10^{-2} \text{ nm}. \tag{15}$$

3.3. Mean physical diameter

After processing the TEM image of the ferrofluid (figure 5(a)) we have obtained the distribution according to the physical diameters d of the nanoparticles, as shown in figure 5(b). According to figure 5(a), the nanoparticles appear roughly spherical. Fitting the experimental values with a log-normal function (full curve) we have found that this curve is well suited to describe the distribution of the particles' diameters. This way we have obtained the distribution parameters $d_0 = 12.6$ nm and $\lambda = 0.10$. By using the relations for calculating the mean diameter, it results that

$$\langle d \rangle = d_0 \exp(\lambda^2/2) = 12.7 \pm 0.1 \text{ nm}. \tag{16}$$

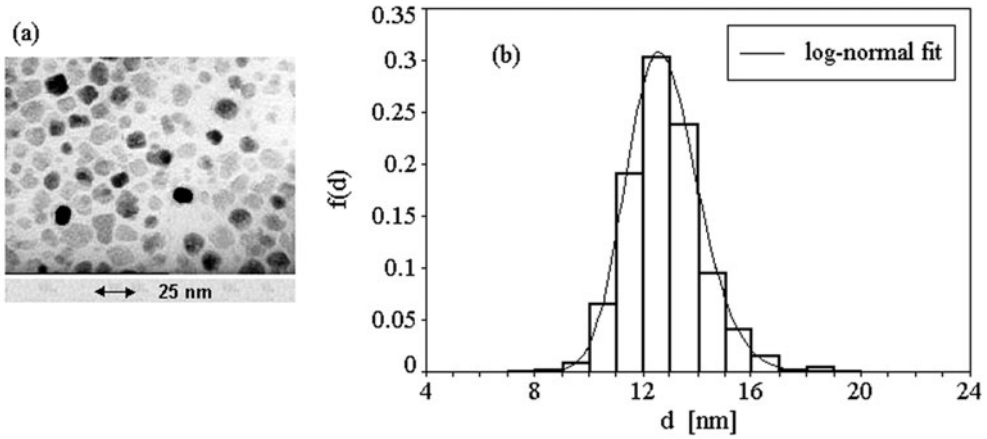

Figure 5. (a) Electron micrograph of the sample. (b) Histogram of the particle diameters.

According to equations (15) and (16), the mean magnetic diameter $\langle d_m \rangle$ deduced from magnetic measurements is smaller than the mean physical diameter $\langle d \rangle$ deduced from the TEM. The results clearly demonstrate that there is a layer at the particles' surface and this layer has a thickness $\langle \eta \rangle = (\langle d \rangle - \langle d_m \rangle)/2 = 0.92 \pm 9.5 \times 10^{-2}$ nm. The value we have obtained for $\langle \eta \rangle$ is in good agreement with the values obtained by other authors [21, 22]. The superficial layer appears as a result of the adsorption of oleic acid molecules (the polar end—COO—of the molecule) at the particles' surface, a process that also has, as a result, the formation of an iron oleate. At room temperature this layer has *no magnetic ordering*. Besides proving the existence of the layer with no magnetic ordering at the nanoparticles' surface, this fact also demonstrates that the values of the diameter $\langle d \rangle$ (deduced from the TEM) and $\langle d_m \rangle$ (deduced from the magnetic granulometric analysis) were determined correctly.

3.4. The modified law in T^2

In agreement with equations (6) and (11), if we take into consideration the mean magnetic diameter $\langle d_m \rangle$, the saturation magnetization of the ferrofluid can be written as

$$M_{sat} = n\pi M_s \langle d_m \rangle^3 / 6. \tag{17}$$

According to equation (17), the relative increase by ∼50% of the mean saturation magnetization of the system made up of surfacted magnetite nanoparticles with the decrease in temperature from 300 to 77 K is attributed to the *increase of the mean magnetic diameter* $\langle d_m \rangle$, attached to the ferrimagnetically ordered cores of the particles because $n =$ constant and M_s has a relatively low increase with the decrease in temperature. If we apply equation (17) at a temperature of 300 K and then at another temperature T ($T < 300$ K), we obtain the following relation:

$$\langle d_m \rangle_T = \langle d_m \rangle_{300} [(M_s)_{300}/(M_s)_T]^{1/3} [(M_{sat})_T/(M_{sat})_{300}]^{1/3} \tag{18}$$

which allows a calculation of the mean magnetic diameter $\langle d_m \rangle_T$ at various temperatures (the index represents the value of the temperature). This way, with the values measured (■) for $M_{sat}(T)$ (figure 2) and the values known for $M_s(T)$ (equation (2)), we have found the values of $\langle d_m \rangle_T$ shown in figure 6(a), curve (■). It can be clearly observed that the mean magnetic diameter increases from 10.86 nm (at 300 K) to 12.4 nm (at 77 K). At the same time, the value of the mean magnetic diameter $\langle d_m \rangle_{77}$ that was determined at 77 K does not exceed the value of

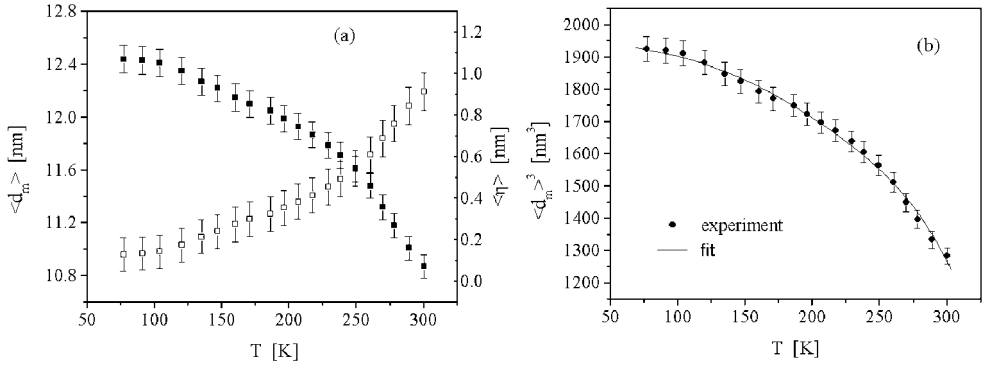

Figure 6. (a) Variation with temperature of the mean magnetic diameter (■) and the thickness of the paramagnetic layer (□). (b) $\langle d_m \rangle^3$ versus T.

the mean physical diameter $\langle d \rangle$ (12.7 nm) that resulted from the TEM. This result represents an additional proof that the significant increase of the magnetization $M_{sat}(T)$ (with the decrease in temperature) can be accounted for by the increase in the nanoparticles' diameter $\langle d_m \rangle$.

The increase of the mean magnetic diameter with the decrease in temperature has, as an effect, the narrowing of the thickness of the layer at the particles' surface according to the formula: $\langle \eta \rangle_T = (\langle d \rangle_T - \langle d_m \rangle_T)/2$. Taking into consideration the values determined for $\langle d_m \rangle_T$, we have calculated the values of $\langle \eta \rangle_T$, with their respective error bars for each temperature. These are shown in figure 6(a), curve (□). When the temperature decreases from 300 to 77 K, the layer on the surface of the nanoparticles narrows by $\langle \eta \rangle^* = (\langle d_m \rangle_{77} - \langle d_m \rangle_{300})/2 = 0.8 \pm 0.1$ nm. This result makes us admit that the layer that is formed at the nanoparticles' surface due to the adsorption of the oleic acid molecule is *paramagnetic* at room temperature. The existence of a paramagnetic layer on the surface of the ferrimagnetic nanoparticles of $Mn_xFe_{3-x}O_4$ ($0.1 < x < 0.7$) in a ferrofluid and covered in oleic acid (as in our case) was recently pointed out by Upadhyay *et al* [36, 37] through electron spin resonance (ESR). Besides the adsorption line that results from the ferrimagnetic core, the line $g = 4$ was observed (g is the spectroscopic splitting factor); the latter one resulted from the Fe^{3+} complex attached to the surfactant molecules. At low temperatures this line disappears. Similarly, Tronc *et al* [38] have shown by means of Mössbauer spectroscopy that, on the surface of phosphated nanoparticles of γ-Fe_2O_3, a paramagnetic layer is formed.

However, our explanation of the reasons that account for the increase in the saturation magnetization with the decrease in temperature in the case of Fe_3O_4 nanoparticles surfacted with oleic acid differs from the explanation given by Morais [19] for the ionic ferrofluid with nanoparticles of $NiFe_2O_4$. Adopting the core–shell model, our explanation is based on the modification of the superexchange interaction between the cations (magnetic ions of Fe–Fe) in the layer on the particles' surface due to the presence of the surfactant molecules. Due to the bonds of the Fe ions at the particles' surface with the O ions from the polar end of the oleic acid molecule, the crystalline lattice from the surface is distorted. The distortion produced by the oleic acid molecules is more intense at the particles' surface and it decreases gradually towards the particles' core. As a result, the ferri–paramagnetic transition temperature (Néel temperature) $T_N \cong W_{ex}/k_B$ (where W_{ex} is the superexchange energy) [39] of the sublayers at the surface that are adjacent to the magnetic core decreases below 300 K. For this reason, the layer at the nanoparticles' surface is paramagnetic at room temperature. While decreasing, the temperature T will gradually become lower than the transition temperatures $T_{N1}, T_{N2}, \ldots$ of the

sublayers $s_1, s_2, \ldots$ (where s_1 is the first sublayer next to the core), $T < T_{N1}$, $T < T_{N2}, \cdots$, and thus the sublayers will in turn become ferrimagnetically ordered (the thermal agitation energy $k_B T$ will become lower than the energy of the superexchange interaction in each sublayer and the atomic magnetic moments will be aligned). Consequently, the volume of the magnetic core where the spins are aligned as a result of the superexchange interaction will increase gradually with the decrease in temperature (figure 6(b), curve (■)). Also, the paramagnetic layer on the nanoparticles' surface will become narrower (figure 6(a), curve (□)). The increase in the magnetic volume has, as an effect, the increase of the magnetic moment m_p and, implicitly, an increase of the saturation magnetization of the nanoparticle system (figure 2, curve (■)).

Based on the results presented above, the law in T^2 for the system made up of surfacted nanoparticles has to be expanded by a term that reflects the increase in the magnetic diameter with the decrease in temperature. Since the magnetic diameter depends on the temperature ($\langle d_m(T)\rangle$), implicitly the magnetic packing fraction will be a function of temperature: $\Phi_m(T)$. In agreement with equation (17), we obtain

$$\Phi_m(T) = M_{sat}(T)/M_s(T) = \pi n \langle d_m(T)\rangle^3/6. \tag{19}$$

Under these conditions, the saturation magnetization of the nanoparticle system $M_{sat}(T)$ can be written as

$$M_{sat}(T) = M_s(T)_{Fe_3O_4}\Phi_m(T). \tag{20}$$

Consequently, in the case of surfacted nanoparticles, the parameter A in equation (1) will not be a *constant*, but a *function of temperature* T. Fitting the values (●) for $(\langle d_m(T)\rangle)^3$ (figure 6(b)) the resulting polynomial function

$$\langle d_m(T)\rangle^3 = \sum_{j=0}^{4} c_j T^{2j} \tag{21}$$

is well suited to describe the variation with temperature. The values of the coefficients c_j are known—they result as fitting parameters. Thus, according to equations (19)–(21), the temperature variation of the saturation magnetization of the system made up of surfacted Fe_3O_4 nanoparticles is described by the law in T^2:

$$M_{sat}(T) = (\pi n M_s(0)_{Fe_3O_4}/6)\left(\sum_{j=0}^{4} c_j T^{2j}\right)(1 - BT^2) \tag{22}$$

and the function

$$M_{sat}(T) = F(T)(1 - BT^2), \tag{23}$$

respectively. In equation (23), $F(T) = A\Phi_m(T) = M_s(0)_{Fe_3O_4}\Phi_m(T)$.

In figure 2(a), the full curve (f3) represents the fit of the experimental values (■) of the saturation magnetization with the function (22), where we have considered the known values for $M_s(0)_{Fe_3O_4}$ (equation (3)), $B \equiv B_{Fe_3O_4}$ (equation (4)) and $n = 3.27 \times 10^{22}$ m^{-3} (where c_j are known constants that were previously determined). The particle concentration in the ferrofluid was calculated with relation (17). It can be observed that there is a very good agreement of curve (f3) with the experimental curve (■). These results confirm the validity of the law in T^2 (22) and (23), respectively, which we have suggested for describing the temperature dependence of the saturation magnetization of the Fe_3O_4 nanoparticles covered in oleic acid. This law takes into consideration the volume increase of the particles' magnetic cores ($\langle V_m\rangle = \pi\langle d_m\rangle^3/6$), where the spins are ferrimagnetically aligned, with the decrease in temperature.

Our previous results [20] have shown that, in the case of *surfacted* $Mn_{0.6}Fe_{0.4}Fe_2O_4$ nanoparticles (in oleic acid), the variation of the saturation magnetization with temperature is very different from the one corresponding to bulk ferrite. Additionally, recent studies that we have carried out (soon to be published) show a similar behaviour both in the case of (Ni–Zn)Fe_2O_4 ferrite nanoparticles and in the case of γ-Fe_2O_3 nanoparticles dispersed in an amorphous SiO_2 matrix (obtained with the sol–gel method). At the surface of the nanoparticles embedded in the matrix, a layer is formed due to the particle–matrix interactions. This layer has a thickness of the order of nanometres and it has no magnetic ordering at room temperature, but it becomes ferrimagnetic at lower temperatures. All these results, as well as the results obtained by other authors [36–38] that confirm the presence of the paramagnetic layer on the surface of surfacted nanoparticles, make us believe that the law (22) is universally applicable for surfacted nanoparticles; the value of the temperature exponent and the values of the coefficients c_j depend on the nature of the material of the nanoparticles.

4. Conclusions

The saturation magnetization as a function of temperature for Fe_3O_4 *surfacted* nanoparticles is correctly described by the law $M_{sat}(T) = F(T)(1 - BT^2)$, which contains the parameter $F(T)$ that depends on the temperature [$F(T) = A\Phi_m(T)$], and not on the law in T^2 verified for bulk magnetite, where $F \equiv A =$ constant ($A = M_s(0)_{Fe_3O_4}$). $F(T)$ as a function of temperature appears as a result of the existence of the layer on the nanoparticles' surface, a layer that is paramagnetic at room temperature. When the temperature decreases below 300 K, the paramagnetic layer gradually becomes ferrimagnetically ordered, starting from the particle's core and moving towards the particle shell. This behaviour is caused by the modification of the superexchange interaction between iron ions from the surface layer of the nanoparticles. Based on the experimental results, we have established that the most suitable function to describe the dependence M_{sat} versus T of the surfacted magnetite nanoparticles in the temperature range of (77–300) K is $M_{sat}(T) = (\pi n M_s(0)_{Fe_3O_4}/6)\Big(\sum_{j=0}^{4} c_j T^{2j}\Big)(1 - BT^2)$.

References

[1] Dormann J L, Fiorani D, Cherkaoui R, Tronc E, Lucari F, D'Orazio F, Spinu L, Noguès M, Kachkachi H and Jolivet J P 1999 *J. Magn. Magn. Mater.* **203** 23

[2] Aliev F G, Correa-Duarte M A, Mamedov A, Ostrander J W, Giersig M, Liz-Marzán L M and Kotov N A 1999 *Adv. Mater.* **11** 1006

[3] Berkowitz A E, Kodama R H, Makhlouf S A, Parker F T, Spada F E, McNiff E J Jr and Foner S 1999 *J. Magn. Magn. Mater.* **196/197** 591

[4] Coey J M D 1971 *Phys. Rev. Lett.* **27** 1140

[5] El-Hilo M, Chantrell R W and O'Grady K 1998 *J. Appl. Phys.* **84** 5114

[6] Hrianca I, Caizer C and Schlett Z 2002 *J. Appl. Phys.* **92** 2125

[7] Hrianca I, Caizer C and Schlett Z 2002 *V. J. Nanoscale Sci. Technol.* **6** webpage http://www.vjnano.org/

[8] Caizer C 2002 *Int. Conf. on Adv. Mater. and Structures (AMS 2002) (Timisoara, 2002)* Contribution: P-2.14 (Providence, RI: American Mathematical Society) p 33

[9] Kodama R H, Berkowitz A E, McNiff E J Jr and Foner S 1996 *Phys. Rev. Lett.* **77** 394

[10] Mollard P, Germi P and Rousset A 1977 *Physica* B **86–88** 1393

[11] Martinez B, Roig A, Molins E, González-Carreño T and Serna C J 1998 *J. Appl. Phys.* **83** 3256

[12] Caizer C and Stefanescu M 2002 *J. Phys. D: Appl. Phys.* **35** 3035

[13] Dillon J F 1962 *Landolt–Börnstein New Series* Group III vol 2(9) (Berlin: Springer) ch 29 pp 50–1

[14] Aldred A T and Frohle P H 1972 *Int. J. Magn.* **2** 195

[15] Aldred A T 1975 *Phys. Rev.* B **11** 2597

[16] Hendricksen P V, Linderoth S and Lindgard P A 1992 *J. Magn. Magn. Mater.* **104–107** 1577

[17] Linderoth S, Balcells L, Labarta A, Tejada J, Hendricksen P V and Sethi S A 1993 *J. Magn. Magn. Mater.* **124** 269
[18] Martinez B, Roig A, Obradors X, Molins E, Claret P and Monty C 1996 *J. Appl. Phys.* **79** 2580
[19] Morais P C, Teixeira C B, Skeff Neto K, Azevedo R B, Lacava Z G B and Lacava L M 2000 *Solid State Commun.* **114** 59
[20] Caizer C 2002 *Solid State Commun.* **124** 53
[21] Rosensweig R E 1985 *Ferrohydrodynamics* (Cambridge: Cambridge University Press)
[22] Raikher Yu I and Shliomis M I 1994 *Adv. Chem. Phys.* **87** 3
[23] Zijlstra H 1967 *Experimental Methods in Magnetism* (Amsterdam: North-Holland) p 103
[24] Smit J and Wijn H P J 1959 *Ferrites* (New York: Wiley) p 156
[25] Jacobs I S and Bean C P 1963 *Magnetism* vol 3, ed G T Rado and H Suhl (New York: Academic) p 271
[26] Kneller E 1962 *Ferromagnetismus* (Berlin: Springer) p 422
[27] Söffge F and Schmidbauer E 1981 *J. Magn. Magn. Mater.* **24** 54
[28] Charles S W 1995 *Rom. Rep. Phys.* **47** 249
[29] Morozov K I 1987 *Bull. Acad. Sci. USSR, Phys. Ser.* **51** 32
[30] Cebers A 1990 *J. Magn. Magn. Mater.* **85** 20
[31] Buyevich Yu A and Ivanov A O 1993 *Physica* A **190** 276
[32] O'Grady K and Bradbury A 1994 *J. Magn. Magn. Mater.* **39** 91
[33] Yaacob I I, Nunes A C and Bose A 1995 *J. Colloid Interface Sci.* **171** 73
[34] Moumen N and Pileni M P 1996 *Chem. Mater.* **8** 11128
[35] Bacri J C, Perzinski R, Salin D, Cabuil V and Massart R 1986 *J. Magn. Magn. Mater.* **62** 36
[36] Upadhyay R V, Srinivas D and Mehta R V 2000 *J. Magn. Magn. Mater.* **214** 105
[37] Sastry M D, Babu Y, Goyal P S, Mehta R V, Upadhyay R V and Srinivas D 1995 *J. Magn. Magn. Mater.* **149** 64
[38] Tronc E, Ezzir A, Cherkaoui R, Chanéac C, Noguès M, Kachkachi H, Fiorani D, Testa A M, Grenèche J M and Jolivet J P 2000 *J. Magn. Magn. Mater.* **221** 63
[39] Valenzuela R 1994 *Magnetic Ceramics* (Cambridge: Cambridge University Press) ch 4